https://doi.org/10.17221/159/2024-CJFS

Study on the geographical origin and characteristic differential components of Qianbei Ma lamb based on rapid evaporative ionization mass spectrometry

Ji Zhang[1], Rui Hou[1], Yuhang Luo[1], Xiaohong Zhang[2], Hong Luo[1], Lei Ling[1], Liping Xiang[1]**

[1]*Zunyi Product Quality Inspection and Testing Institute, Zunyi, China*
[2]*College of Pharmacy, Zunyi Medical University, Zunyi, China*

**Corresponding authors: 1248856128@qq.com; 1090479476@qq.com*

Citation: Zhang J., Hou R., Luo Y., Zhang X., Luo H., Ling L., Xiang L. (2025): Study on the geographical origin and characteristic differential components of Qianbei Ma lamb based on Rapid Evaporative Ionization Mass Spectrometry. Czech J. Food Sci., 43: 59–70.

Abstract: A rapid evaporative ionization mass spectrometry (REIMS) method combined with intelligent knife (iKnife) method was developed to explore the geographical origin and characteristic differential components of Qianbei Ma lamb. The REIMS conditions were initially refined, with the cauterization duration of 3 seconds, and the auxiliary solvent flow rate set to 100 μL·min^{-1} to prevent duplication. A database model was created from raw data through the proposed principal component analysis-linear discriminate analysis (PCA-LDA) in Live ID software, successfully applied to identify samples from 5 provinces in China and the real-time reliable identification rate with confidence higher than 99%. The obtained data by REIMS were used to establish the multivariate statistical models which using orthogonal projection to latent structures discriminant analysis (OPLS-DA), provided strong the discrimination power between composition and content changes of 16 specific ions such as *m/z* 726.3952 and *m/z* 744.4050, etc., including fatty alcohols, fatty acids and phosphatidylserines in mutton of different origin and the model displayed validation [R^2(Y) = 0.968, Q^2 = 0.924].

Keywords: REIMS; real-time discrimination; Qianbei Ma lamb; different origins; multivariate statistical analysis; chemometrics

Qianbei Ma lamb is a national local fine variety, originally located from the Xishui County, Zunyi City, Guizhou Province in China; now it has become China's national product with geographical indication. In 2020, the Qianbei Ma lamb population in Zunyi City reached 334 500 head, with 236 000 sheep marketed. The total production value was nearly 700 000 USD, benefiting approximately 30 000 households and over 120 000 individuals. However, the contradiction between the best-selling and high market recognition of Qianbei Ma lamb and the current low slaughter volume has led to the existence of hybrid varieties in the market. Currently, such an insufficient supply leads to low-value foreign lamb being more easily obtained in comparison with high-value Qianbei Ma lamb, resulting in unreasonable profits and frequent occurrences of adulterated and counterfeit food. Incidents of adulteration in the market occur frequently, and they are challenging to detect.

Supported by Guizhou Provincial Science and Technology Department Project [Guizhou Science and Technology Support (2022) General 090].

https://doi.org/10.17221/159/2024-CJFS

Therefore, establishing a traceability analysis method for the origin of Qianbei Ma lamb meat is crucial, simultaneously exploring its superior quality.

In recent years, numerous instrumental analysis techniques have been employed to determine the geographical origin. For example, Wang Yan applied isotope analysis methods to trace the origin of Inner Mongolian mutton. Mineral elements in organisms can be categorized into major and trace elements based on their concentrations. By analysing the composition and content variations of these mineral elements in animals, it is possible to identify their origin (Sun 2011; Calvano et al. 2013). Isotope ratio measurements of $^{2}H/^{1}H$, $^{13}C/^{12}C$, $^{15}N/^{14}N$ and $^{18}O/^{16}O$ can accurately indicate the geographical origin, however, they require specialized equipment and typically involve extended preparation and analysis times (Camin et al. 2016). Therefore, there is an immediate need for a simple, rapid, accurate and efficient detection method for screening and monitoring the authenticity of mutton in Qianbei Ma lamb. The drawbacks of these methods include the need for sample transportation to the analytical laboratory, storage requirements, and lengthy, complex sample preparation procedures, expensive equipment, complex analytical protocols, and time-consuming chromatographic separations, all of which require several working days to obtain final results.

In the last decade, there have usually been two suitable methods for rapid analysis: one is a probe electrospray ionization (PESI) technique, where a solid probe is used to collect the sample surface and the liquid phase residues are determined by orthogonal time-of-flight mass spectrometry (Hiraoka et al. 2007). The other is based on an innovative mass spectrometric ionization technique that utilizes rapid evaporation of biological tissues (Hiraoka et al. 2007). Rapid evaporative ionization mass spectrometry (REIMS) is a relatively novel technique for metabolic fingerprinting based on mass spectrometry, able to authenticate or identify mutton according to its different geographical origin (Balog et al. 2016). Our knowledge from searching the literature indicates that the majority of the applications reported from the novel REIMS technology focus on animals (Rigano et al. 2019; Shen et al. 2020) and microorganisms (Bodai et al. 2018; Shen et al. 2019), several studies involving human cancer (St John et al. 2017; Birse and Elliott 2024). Based on these observations, the REIMS technology is anticipated to establish its application niche in food security, particularly in food authenticity and food microbiology (Balog et al. 2016). This REIMS-based technique has been demonstrated to be an effective tool for compound characterization, attributed to its key advantages of speed, sensitivity, high resolution, and experimental simplicity.

The aim of this study was to establish a provenance traceability model and experimental analysis workflow for Qianbei Ma sheep that could enable real-time lamb origin prediction in a matter of minutes (Figure 1). Because the molecular fingerprints generated by REIMS combined with contact heating through intelligent knife (iKnife) analysis can reflect the authenticity of lamb origin, therefore the technology has significant developmental advantages as a rapid assessment tool for geographic origin detection and can provide a reference for adulteration assessment in the marketplace (Cui et al. 2021).

MATERIAL AND METHODS

Reagents and chemicals

Methanol, sodium formate, and the internal standard leucine-encephalin (LE, purity ≥ 97%) were of chromatographic grade and they were sourced by Sigma-

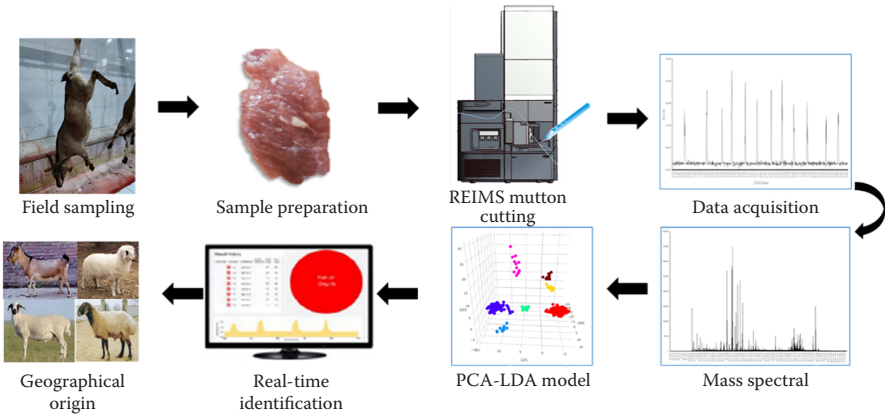

Figure 1. The process diagram on the geographical origin of Qianbei Ma lamb based on rapid evaporative ionization mass spectrometry (REIMS)

https://doi.org/10.17221/159/2024-CJFS

Aldrich (Sigma-Aldrich Shanghai, Trading Co Ltd., China), LE was supplied by Waters (Waters Corporation Shanghai, China). Deionized water with a resistivity of 18.2 MΩ·cm was acquired using a Milli-Q system (Merck, Millipore, USA).

Sample preparation

A total of 124 samples of Qianbei Ma lamb and 50 samples of lamb from other provinces were collected, including 15 lamb samples from Ningxia, 12 lamb samples from Gansu, 12 lamb samples from Inner Mongolia, and 11 lamb samples from Xinjiang. The information on the mutton used in the experiment is listed in Table 1. The out-of-province lamb samples were purchased from the official flagship store of online shopping platform, and Qianbei Ma lamb samples were provided by local farmers for on-site sampling. To maintain consistency and authenticity of each sample, all the samples were collected by special personnel from the same position on the lamb leg. Each lamb sample was sectioned into small fragments of approximately 5 × 4 × 2 cm and stored in a frozen dumpling box. Fresh lamb samples were stored in plastic wrap at –20.0 ± 0. 5 °C, thawed at 4 ± 0. 5 °C for 4 h when needed, and placed neatly on tinfoil.

Rapid evaporative ionization mass spectrometry analysis

The iKnife portable sampling instrument (Waters Corporation, USA) works by electrosurgical evaporation of the aerosol containing gaseous compounds via a Venturi pump, by a 4 m × 3.9 7 mm outer diameter (o.d.), 2.3 8 mm inner diameter (i.d.), Tygon PVC smoke evacuation line and is detected by Quadrupole Time-of-Flight Mass Spectrometer (Q-TOF-MS, Xevo G2-XS, Waters Corporation, UK) and real-time mass spectrometric analysis. The iKnife received power from an Erbotom ICC 300 (Erbe Elektromedizin GmbH, Germany) electrosurgical generator, which delivered a controlled sinusoidal 33 0 kHz alternating current. The generator operated in 'cut' mode at a power setting of 40 W. To ensure the accuracy of the mass axis, the instrument underwent calibration through the infusion of sodium formate. This process yielded a limited set of potential candidates for each level of the mass accuracy, ultimately achieving a mass accuracy within the range of less than 0.5 ppm in routine applications. To subtract the background from the spectra and perform the lock-mass calibration, leucine encephalin was dissolved in methanol at a concentration of 20 ng·mL^{-1}, serving as an internal reference peak. This solution was introduced into a heated helix collision surface maintained at approximately 750 °C via a stainless steel capillary (1/16' o.d., 0.002' i.d.). In negative ionization mode the lock-mass correction was performed using the lock-mass *m/z* 554.2516 for meat samples. Following this correction, the spectra were normalized to total ion count (TIC) and rebinned to a 0.1 Da interval.

All thawed lamb samples were cut directly with iKnife into burn marks approximately 2 mm deep and 15 mm long, when cutting was repeated approximately 10 times, and then they were combined into 10 replicate spectra with 10 s intervals between each cut. To prevent loss of conductivity and carry-over effects, visible contamination on the inner wall of the 4-meter-long ion transfer tube, as well as on the iKnife blade and components of the ion source, was cleaned in an ultrasonic bath with methanol after every 10 samples. In the absence of this cleaning, the residues were removed by scraping and wiping the knife with a clean tissue. All analyses were conducted in MS sensitivity mode using continuous data acquisition. In negative ionization mode, the mass spectra were acquired over a range of *m/z* 100 to 1 000, comprising 6–8 scans at a mass resolution of 20 000 full widths at half maximum (FWHM) at *m/z* 600. All of the mass spectrometry data were acquired with the instrument control software package MassLynx (version 4.1., Waters Corporation, UK). The

Table 1. Information sheet for experimental mutton samples

Common name	Place of origins	Specimens	Spectra	Enterprise	Acquisition time
Qianbei Ma lamb	Xishui, Guizhou	54	540	qiandao	
Qianbei Ma lamb	Xishui, Guizhou	67	660	fuxing	2022.06–2022.11
Qianbei Ma lamb	Renhuai, Guizhou	3	30	renhuai	
Tan sheep	Ningxia	15	119	online	2022.12
Alpine fine-wool sheep	Gansu	12	110	online	2022.11–2022.12
Sunit lamb	Inner Mongolia	12	118	online	2022.12
Altay big tail sheep	Xinjiang	11	100	online	2022.11–2022.12

https://doi.org/10.17221/159/2024-CJFS

mean value and coefficient of variation (*CV*) of intra-day and inter-day method optimization were calculated using Microsoft Excel software (2021).

Multivariate statistical model

The resulting data vectors were analysed using multivariate statistics to develop a classifier for identifying the species of origin. Background reduction was achieved by the application of the adaptive background subtraction algorithm which was used to set the TIC threshold, then the cut peak was extracted and the leucine encephalin intensity was analysed; this intensity was used to set its threshold. The endogenous matrix ions were calibrated by a lock-mass correction using the internal standard LE (*m/z* 554.2615). Multivariate statistical software package LiveID™ (Waters Corporation, UK) was used for the chemometric model building by principal component analysis (PCA) and linear discriminate analysis (LDA) from the model was developed using the training set samples for the real-time identification of mutton. REIMS data were pre-processed using Progenesis Bridge software (version 2.0, Waters Corporation, UK), which cut individual REIMS raw files into a separate file while subtracting the TIC replicate threshold. The replicates were identified based on the TIC replicate threshold, combining the spectra of the scans of each replicate.

Compound identification

The data for each run stored in a separate raw folder were imported into Progenesis QI (Non-linear Dynamics, UK) for analysis. The chemical identity of the detected ionic species was established using accurate mass information which was processed by Masslynx software (version 4.2). The *m/z* values were identified by comparing the accurate mass measurements with predictions from the LIPIDMAPS tool (www.lipidmaps.org). The data file that possesses common characteristics was selected as the reference file of data alignment which groups adducts that correspond to the same compound and conducts tentative identification by correlating the measured masses with predictions from the LIPIDMAPS tool, using a mass error threshold of 5 ppm. An unsupervised principal component analysis transformation and supervised partial least squares-discriminant analysis (PLS-DA) methods were built through the combination of SIMCA software (version 14.1, Umetrics Sartorius Stedim Biotech, Sweden) and EZInfo to determine candidate biomarkers and analysis on the abundance of identified ions in each sample. Typically, the value of model predictive ability near 1.0 suggests a strong fit and predictive capacity for the model. The R^2 (cumulative) and Q^2 (cumulative) scores were commonly employed to assess the quality and reliability of the statistical model used in this study.

RESULTS AND DISCUSSION

Optimization of rapid evaporative ionization mass spectrometry experimental conditions

Previous research has verified that the primary physical factor influencing REIMS was the rate of heating (Balog et al. 2016). As a thermally driven process, the mechanism of rapid evaporative ionization using an iKnife is related to heat generation and transfer during the cutting process (Schäfer et al. 2009). To ensure stable and reliable data from the collected lamb samples, the experimental parameters for REIMS were optimized, encompassing cutting speed, cutting distance, auxiliary solvent flow rate, and power output. The characterized lipid ion peaks were selected as representative indices, including two fatty acid ions (*m/z* 279.2317 and 281.2495) and four phospholipid ions (*m/z* 681.4830, 699.5001, 726.5416, and 863.5609) as the target objectives to validate parameters such as cutting speed of the monopolar electrode handpiece, power output of energy device, and cutting distance of the monopolar electrode handpiece in the conducted pre-experiment. Using the univariate method to optimize the experimental procedure, the initial parameters were determined as a cutting speed of 4 mm·s^{-1}, cutting voltage of 20 V, cutting distance of 10 mm, and LE flow rate of 50 μL·min^{-1}.

The results showed that the response of the selected ions rose as the LE flow rate was accelerated from 50 to 100 μL·min^{-1}, and it decreased gradually after that (Figure 2A). In addition, a flow rate of 100 μL·min^{-1} was demonstrated to be adequate for maintaining the diversity and resolution of the ions. The change in cutting speed was tested ranging from 4 to 10 mm·s^{-1}, while the other conditions were fixed, and the results are shown in Figure 2B. The results showed that the peak areas of the selected ions increased with the enhancement of cutting speed from 4 to 6 mm·s^{-1} and decreased thereafter while the highest peak areas were produced at 6 mm·s^{-1}. The impact of the cutting distance on the ion intensities was evaluated from 10 to 25 mm. As shown in Figure 2C, the signal-to-noise ratio decreased as the ionization of compounds on the surface of muscle samples occurred when the power

https://doi.org/10.17221/159/2024-CJFS

output of the generator was changed from 20 to 50 W. As shown in Figure 2D, the maximum intensities of the six ions were recorded at a cutting distance of 25 mm. The signal-to-noise ratio decreased when the power was too high, mainly because the high energy leads to more radicals. Based on the aforementioned optimization results, the cutting speed, cutting distance, auxiliary solvent flow rate and power output were established at 6 mm·s^{-1}, 25 mm, 100 µL·min^{-1} and 20 W, respectively, for the subsequent experiments.

Precision of REIMS

The three leg muscle samples (coded KY447-449) were each replicated six times and the response values of the characterized lipid ions were recorded using REIMS in negative ionization mode as a minimum of triplicates on three consecutive days. *CV* is a statistical measure of the relative variability of a data set. It expresses the ratio of the standard deviation to the mean, allowing for the comparison of variability across different data sets, especially when the data sets have different units or scales.

The results are as follows in Table 2: the intra-day accuracy for fatty acid and phospholipid ion peaks is 6.8% to 12.7%. Meanwhile, the inter-day reproducibility values range from is 7.9% to 21.4%. These results collectively highlight the precision and consistency of the REIMS method in the analysis of fatty acids and phospholipids, providing valuable insights into the reliability of the proposed approach.

Mass spectra identification and characterization

Integrating findings from the literature with experimental results showed that the MS profiles of different origin were acquired in negative ion mode by iKnife REIMS. Each meat pieces of dimensions 5 × 4 mm was cut 10 times using an iKnife, and the length of the cuts was 15 mm. A representative TIC chromatogram and mass spectrum are shown in Figure 3; there was little variation in the accurate mass information across the different acquisitions. The REIMS spectra consist-

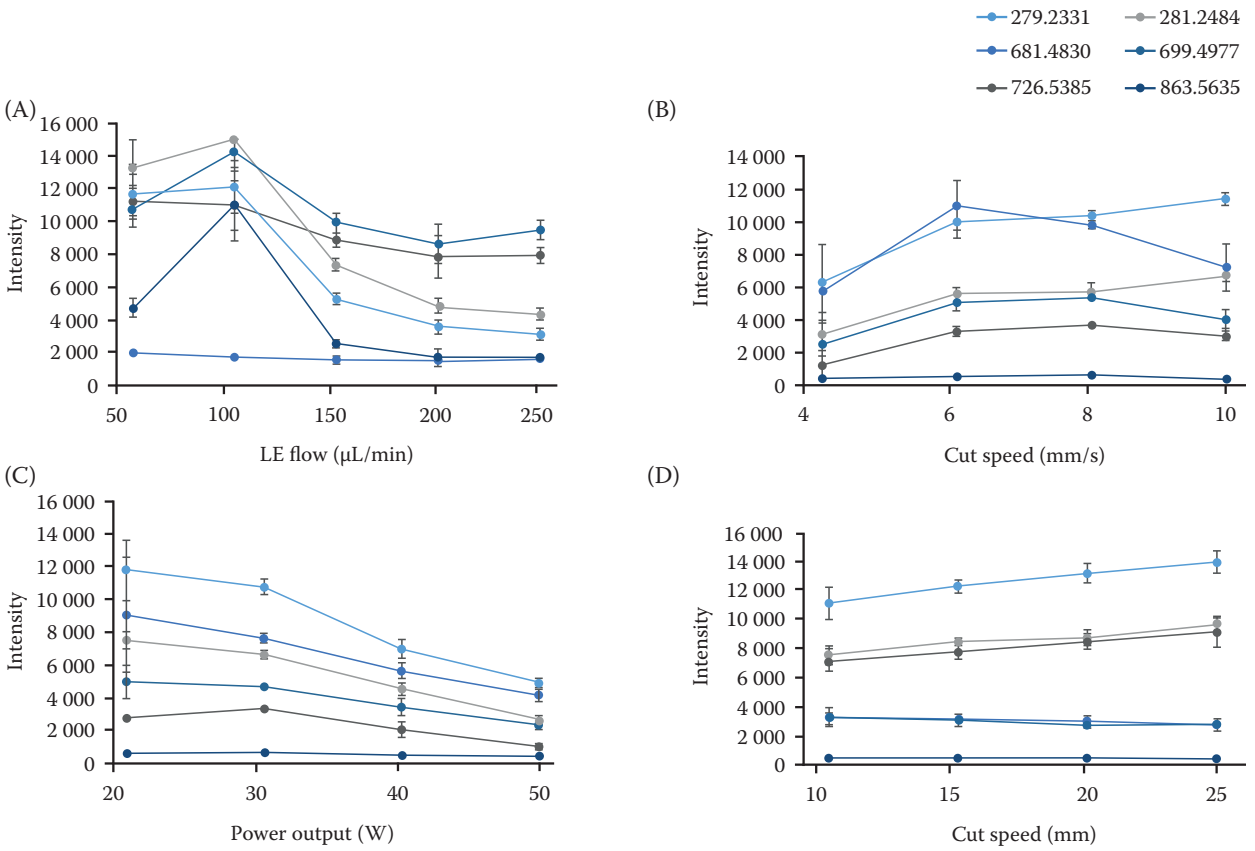

Figure 2. Effect of (A) flow rate of internal standard solvent, (B) cutting speed of monopolar electrode handpiece, (C) power output of energy device, and (D) cutting distance of monopolar electrode handpiece on the peak areas of selected fatty acid ions and phospholipid ion

LE – leucine-encephalin

https://doi.org/10.17221/159/2024-CJFS

Table 2. The accuracy and reproducibility of the method proposed by rapid evaporative ionization mass spectrometry (REIMS) were assessed using the selected ion peaks of fatty acids and phospholipids

Ion peaks (*m/z*)	Chain composition	Chemical class	Intra-day	Inter-day
			proportion *CV* (%)	reproducibility *CV* (%)
279.2317	18:2	fatty acid	9.8	21.4
281.2495	18:1	fatty acid	11.2	20.7
681.4830	PA O-36:4	phospholipids	12.7	17.8
699.5001	PA 36:2	phospholipids	8.9	14.1
726.5424	PE P-18:0/18:2	phospholipids	6.8	7.9
	PC 14:0/18:1	phospholipids		
279.2317	PI (19:1(9Z)/17:0)	phospholipids	9.8	21.4

PA – phosphatidic acid; PE – phosphatidylethanolamine; PC – phosphatidylcholine, PI – phosphatidylinositol; O (O-36:4) – oxygen which is a simplified form to refer to the position where an oxygen atom is connected; P (P-18:0/18:2) – phosphorus which is a simplified form to refer to the position where phosphorus atom is connected

ed of characteristic ions primarily located within the mass-to-charge (*m/z*) ranges of 250–450 and 500–900, corresponding to two distinct types of molecular species: fatty acids and phospholipids, respectively. The signals associated with fatty acid ions may arise from the ionization of free fatty acids and/or the fragmentation of phospholipids (Rui et al. 2010; Shen et al. 2019).

Reference-prepared mutton was analysed from each origin using identical instrumental conditions. The REIMS fingerprints indicated that spectral data from five mutton samples of different origins were predominantly characterized by intact phospholipids and fatty acids (Black et al. 2017). Figure 3 presents the expansion of the fatty acid (FA) region (250–450 *m/z*) and the phospholipid region (PLs) (500–900 *m/z*), along with the identification of the primary components. The data indicate nearly identical profiles in the FA region across different samples, particularly among all lamb species. For instance, *m/z* 325.1887 and *m/z* 339.2018 represented the most abundant species in the acquired spectra (Figure 4A), whereas the range from *m/z* 660 to *m/z* 800 was the least abundant in the spectra shown in Figure 4B.

Model establishment and traceability

A multivariate model (Figure 5) was built from 172 mutton samples; a total of 1 650 original mass spectra data points including 1 240 Qianbei Ma lamb, 119 Ningxia lamb, 110 Gansu lamb, 118 Inner Mongolia lamb, and 100 Xinjiang lamb were pretreated, and an additional multivariate statistical analysis was performed. The PCA-LDA analysis model typically consists of the first 25 principal components, which are tested by building the *in silico* stratified fivefold cross-validation, where four partitions (80%) are used to develop the original model, while the final subset (20%) serves as a training set for recognition during playback. Among 1 650 original mass spectra data

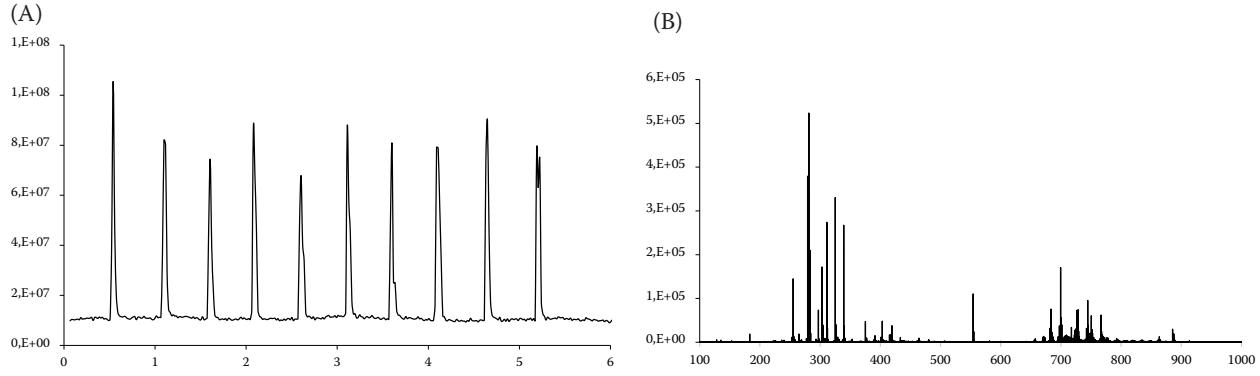

Figure 3. (A) Representative total ion count (TIC) chromatogram, and (B) mass spectrum of mutton sample

https://doi.org/10.17221/159/2024-CJFS

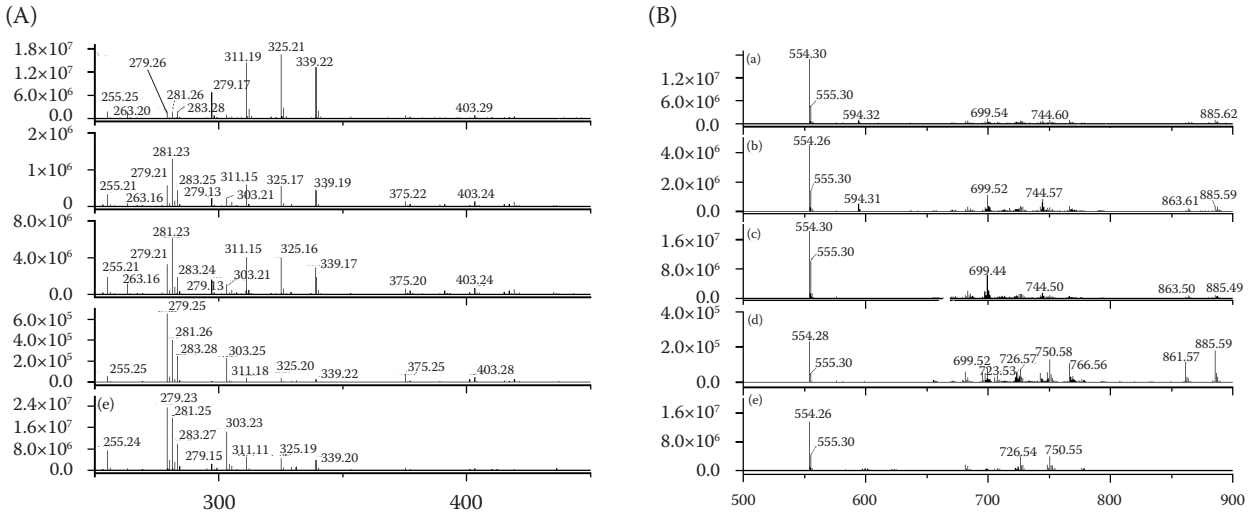

Figure 4. Comparison of the rapid evaporative ionization mass spectrometry (REIMS) mass spectrum of fatty acids (A) in the *m/z* range of 250–450 and phospholipids (B) in the *m/z* range of 500–900 acquired from each lamb origin for a) Qianbei Ma lamb, b) Xinjiang, c) Neimenggu, d) Ningxia, e) Gansu

points, 1 491 data points passed successfully, 156 data points failed, and 3 data points were not identified. The validation of this PCA-LDA model achieved a correct classification rate of 90.36%, and it includes the total counts of correct and incorrect classifications, along with the number of outliers, which theoretically suggests its high accuracy in predicting the identification of lamb of different origins. The ultimate purpose of building the model is to identify the geographical origin of Qianbei Ma lamb in the production process and circulation field. After predicting the model accuracy through the *in silico* validation, its performance was further tested by the proposed REIMS method in which the experimenter randomly selected 30 authentic Xishui Ma sheep random blind samples from the breeding enterprises (not included in the training data set). The software provided real-time results for the accurate identification of Qianbei Ma lamb, suggesting that at least three replicates of tentative identifications should be considered for the experimental validation of the model. Among all identification results, 2 samples were unidentified, while 28 samples were correctly identified, some were identified incorrectly, resulting in an overall real-time identification accuracy of 93.3%. Due to the absence of established standards for the REIMS technology used in this study, it is difficult to compare the identification accuracy with similar methods. However, compared to other detection techniques (pulsed electrospray ionization PESI; ion mobility spectrometry IMS, etc.) the REIMS method in this study demonstrates the relatively higher identification accuracy, indicating its potential application value.

The multivariate statistical analysis was used to quickly identify the disparity observed in the spectroscopic data obtained from the REIMS analysis of mutton samples. A total of 72 representative samples with good parallelism and stable response in the total ion current diagram for the model establishment were used for orthogonal partial least squares discriminant analysis (OPLS-DA) modelling, including 40 samples of Qianbei Ma sheep and 32 samples of other sheep (8 samples each from Gansu sheep, Inner Mongolia sheep, Xinjiang sheep, and Ningxia sheep). The model utilized automatic fitting. The score plot generated from OPLS-DA (Figure 6A) was established to identify significant differences between the two groups of related metabolite information, the selection criteria were set as follows: max fold change ≥ 2, PLS-DA variable importance in projection (VIP) > 1, minimum $CV \geq 30$, and analysis of variance probability-value (ANOVA P– value) ≤ 0.05 and regularly used R^2 and Q^2 to evaluate the quality and reliability of these models. The results indicate that the models exhibited strong applicability and predictive capability [$R^2(Y) = 0.968$, $Q^2 = 0.924$], with $R^2(Y)$ assessing applicability and Q^2 reflecting predictive ability. Their values approaching 1.0 suggest the excellent model fit and predictive performance. A Q^2 value greater than 0.5 was considered indicative of good predictivity for the biological models (Wilde et al. 2019).

https://doi.org/10.17221/159/2024-CJFS

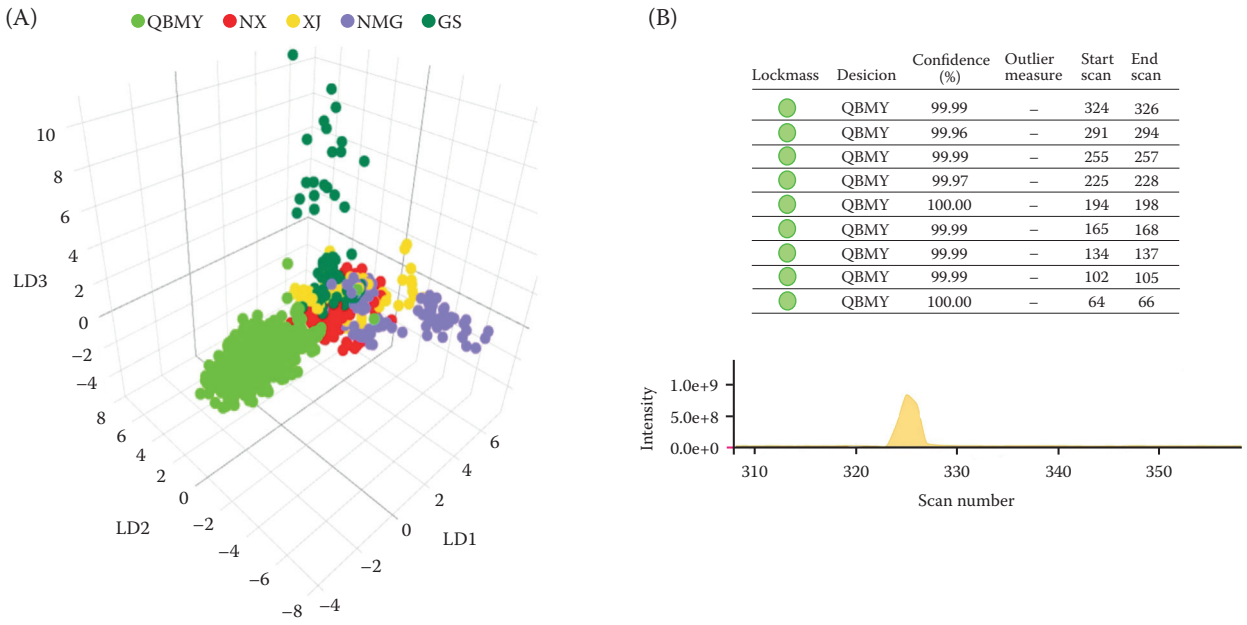

Figure 5. (A) PCA-LDA score plots of the optimized geographical origin model were generated using LiveID and (B) real-time identification of QBMY sample

Statistical analysis and candidate differential *m/z*; PCA-LDA – principal component analysis-linear discriminate analysis; QBMY – Qianbei Ma lamb; GS – Gansu; XJ – Xingjiang; NX – NingXia; NMG – Neimenggu

The potential presence of outliers within the model was identified using Hotelling's T^2 (T-squared statistic) plot (Figure 6B). Observations falling within the 95% and 99% confidence limits were classified as suspect and strong outliers, respectively (Verplanken et al. 2017; Liu et al. 2018). No samples exceeded the model limit (T^2crit 99%), and only one sample was found beyond the model limit (T^2crit 95%), which was considered a suspect outlier and could be retained in the model.

To illustrate the characteristic ions that differentiate the various origins, the S-line (Figure 6C) was created, indicating that the vertical axis represents the contribution [p(ctr)] of specific ions to the correlation [p(corr)] of the observations. In metabolomics studies aimed at revealing qualitative profiles, high-resolution mass spectrometry (MS) systems combined with specialized software are commonly used. This software is intended to compare MS data with information available in online and/or commercially accessible databases.

According to the OPLS-DA model, the biomarkers were selected based on the outcomes of the VIP analysis. There were twenty-eight ions (VIP > 2) and one hundred and fifty-two ions (VIP > 1) with high correlation values that were considered indicative of the characteristic ions used for authenticating the geographical origin. The ion with the greatest influence was *m/z* 587.5002 ($C_{38}H_{64}O_2$), followed by *m/z* 583.4692 ($C_{37}H_{60}O_5$), *m/z* 575.4411 ($C_{31}H_{61}O_7P$), and *m/z* 554.4939 ($C_{34}H_{69}NO_4$). For an OPLS model, SIMCA displays scaled and centred coefficients pertaining to the predictive components that are shown in the coefficient plot (Figure 6D). Overall, the identified *m/z* concentrations were increased or decreased in the vertical axis. Mahalanobis squared distance to the closest category centroid was calculated for each class average. If the distance, as previously defined and excluded from data analysis, exceeded the outlier threshold, the sample would be identified as an outlier. The fatty acid composition of the two types of mutton was quite different. In the sample of Qianbei Ma sheep, PS29:1, PE34:5, PA36:8 and DG34:6 were the major fatty acids.

Differences between the two groups were considered significant when both VIP values exceeded 1 and the P-value was less than 0.05. As illustrated in Figure 7, the ions at *m/z* 281.194, 705.485, 253.217, 726.395, 744.405 and 723.358, among others, exerted a noteworthy impact on the dataset and played a crucial role in distinguishing between Qianbei Ma lamb samples and lamb samples of other origins. Hence, these *m/z* were identified as potential markers for discriminating between Qianbei Ma lamb and lamb

https://doi.org/10.17221/159/2024-CJFS

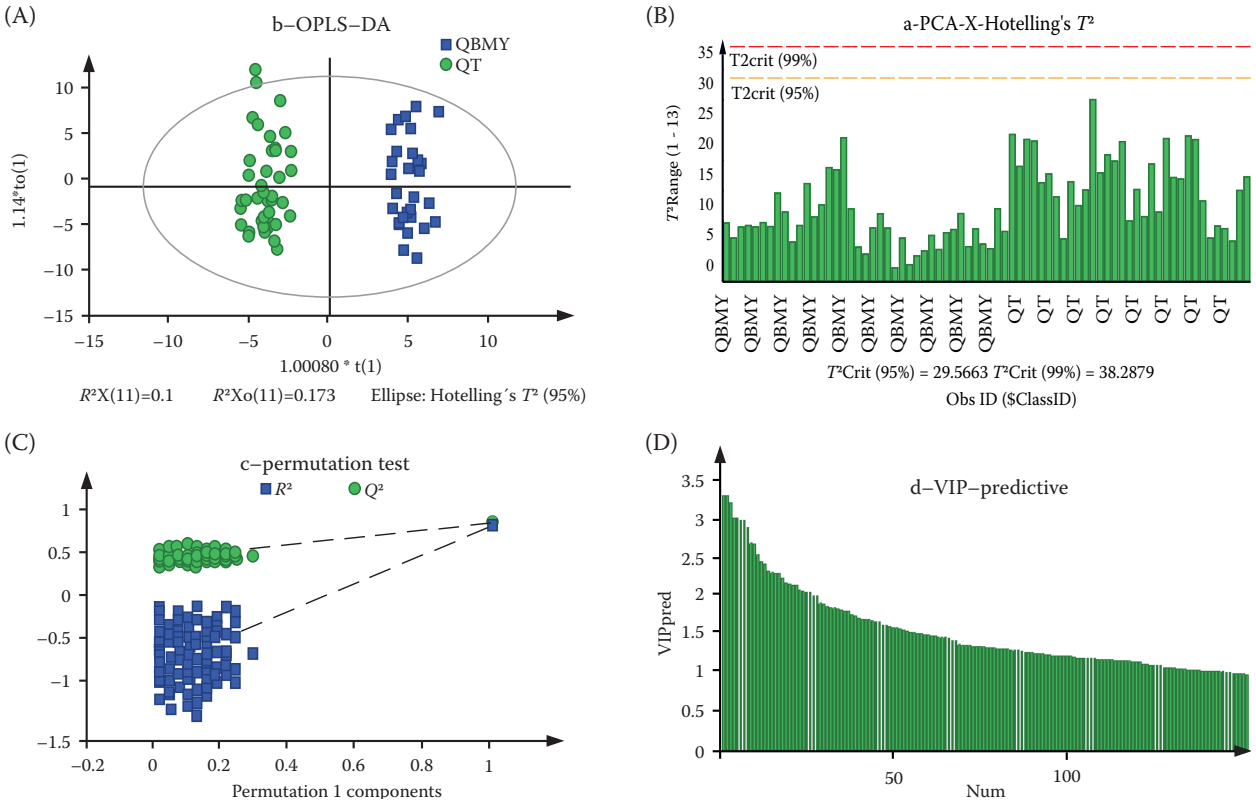

Figure 6. Statistical results of the OPLS-DA model: (A) two-dimensional score plot; (B) Hotelling's T^2 plot; (C) ROC curve for the prediction; (D) the VIP plot

QBMY – Qianbei Ma lamb; QT – other origins lamb; OPLS-DA – orthogonal projection to latent structures discriminant analysis; ROC – receiver operating characteristic; VIP – variable importance in projection

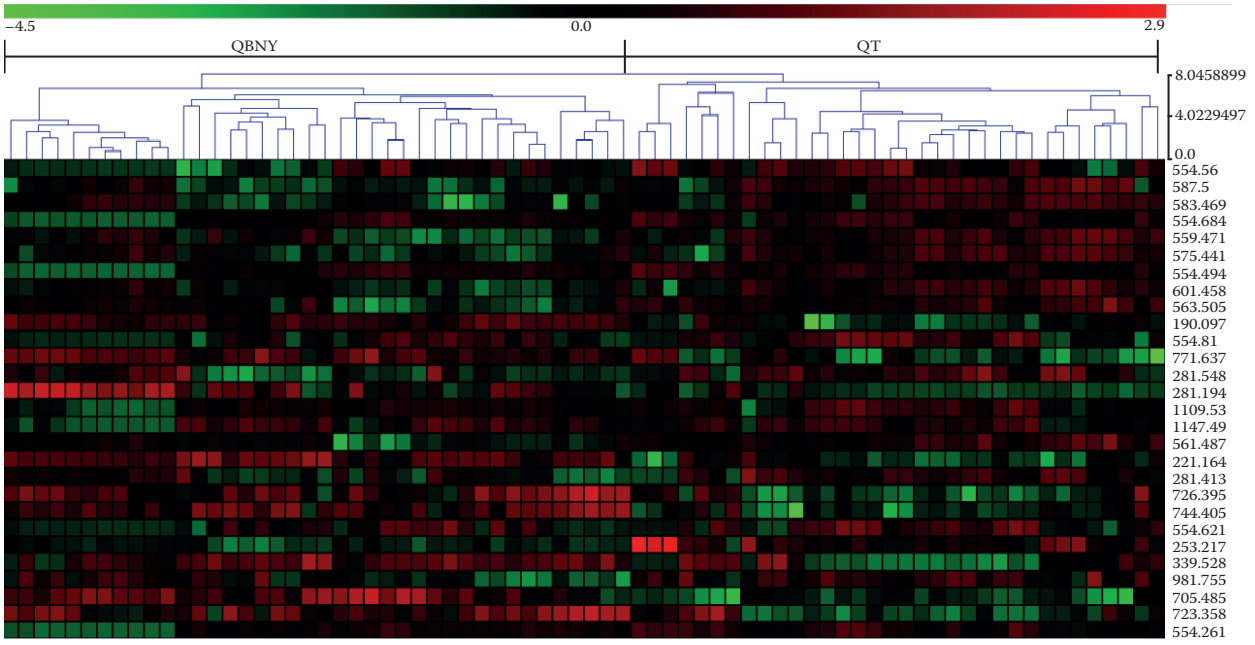

Figure 7. The vertical labels indicate the identified ions, while the horizontal dendrogram depicts the samples

https://doi.org/10.17221/159/2024-CJFS

samples of other origins. Multiple underlying factors contribute to this, including variations in sheep breeds, differences in pastures and supplementary feed, as well as disparities in climatic conditions (e.g., year-round outdoor grazing versus indoor wintering) and slaughter methods.

Based on the literature and preliminary experiments, the spectra acquired from fatty acids and phospholipids during negative ionization were found to be more informative and exhibited a higher ease of ionization compared to positive ionization. In the low *m/z* region, the predominant observation was of deprotonated fatty acid species. Fatty acids were identified based on their precise *m/z* values and information from prior publications (Song et al. 2020).

These ions were primarily identified as fatty alcohol (FOH), fatty acid (FA), ceramide (Cer), diacylglycerol (DG), wax ester (WE), phosphatidic acid (PA), phosphatidylserine (PS), phosphatidylethanolamine (PE), triglyceride (TG), major deprotonated species $[M\text{-}H]^-$ and $[M\text{-}Cl]^-$ (Table 3). As a process relatively high in energy, REIMS has the potential to trigger demethylation and deamination processes in PS and PE, resulting in the detection of $[M\text{-}CH_3]^-$ and $[M\text{-}NH_3]^-$ ions, respectively. The peak assignments in the mass spectra are initial and necessitate further analysis. For other ions displaying low signal intensities, the assignments were determined based on information from prior publications. Notably, in this study, there were notable variations in the levels of PA, PS, and PE. Usually, time-of-flight mass spectrometry is employed for qualitative analysis, while quantitative analysis is not as effective as triple quadrupole mass spectrometry. The identified compounds require further quantification using triple quadrupole mass spectrometry with the acquisition of relevant standard substances to obtain accurate results. This approach not only enables the differentiation of compounds between Qianbei cashmere goats and those from other regions but also it facilitates the analysis of their content levels. It provides theoretical support to further research into the intrinsic components of Qianbei cashmere goats (Zhang et al. 2022).

CONCLUSION

By integrating REIMS with chemometrics, a proficient real-time traceability method was suggested for

Table 3. The probable attribution, adducts, and mass error of compounds in the range of *m/z* 50–1 200 in Qianbei Ma lamb samples and lamb samples of other origins

Significant ion (*m/z*)	Exact ion (*m/z*)	Probable attribution	Adducts	Mass error (ppm)	Elemental composition	Max fold change
221.1638	186.19837	FOH 12:0	$[M\text{-}Cl]^+$	–21.5	$C_{12}H_{26}O$	1.8
253.2166	254.22458	FA 16:1	$[M\text{-}H]^-$	–2.7	$C_{16}H_{30}O_2$	2.4
281.1945	282.25591	FA 18:1	$[M\text{-}H]^-$	–3.5	$C_{18}H_{34}O_2$	2.7
554.4939	555.52266	Cer 34:0; O3	$[M\text{-}H]^-$	–38.7	$C_{34}H_{69}NO_4$	2.3
561.4865	562.45973	DG 32:3	$[M\text{-}H]^-$	60.6	$C_{35}H_{62}O_5$	3.2
563.5045	564.47538	DG 32:2	$[M\text{-}H]^-$	64.4	$C_{35}H_{64}O_5$	3.2
575.4411	540.47538	DG 30:0	$[M\text{-}H]^-$	57.1	$C_{31}H_{61}O_7P$	2.4
583.4692	584.44408	DG 34:6	$[M\text{-}H]^-$	55.5	$C_{37}H_{60}O_5$	7.6
587.5002	552.49063	WE 38:6	$[M\text{-}Cl]^+$	72.6	$C_{38}H_{64}O_2$	4.4
601.4579	566.49103	DG 32:1	$[M\text{-}Cl]^+$	–4.4	$C_{35}H_{66}O_5$	3.1
705.4853	706.49374	PA O-38:6	$[M\text{-}H]^-$	–1.7	$C_{41}H_{71}O_7P$	2.3
723.3583	688.41041	PA 36:8	$[M\text{-}Cl]^+$	–31.2	$C_{39}H_{61}O_8P$	73.3
726.3952	691.44244	PS 29:1	$[M\text{-}Cl]^+$	–24.0	$C_{35}H_{66}NO_{10}P$	294.0
744.4050	709.46826	PE 34:5	$[M\text{-}Cl]^+$	–46.0	$C_{39}H_{68}NO_8P$	170.0
771.6366	772.63459	PA O-42:1	$[M\text{-}H]^-$	12.1	$C_{45}H_{89}O_7P$	3.2
981.7545	946.79894	TG 59:7	$[M\text{-}Cl]^+$	–14.6	$C_{62}H_{106}O_6$	1.8
1147.486	1112.44050	PIP3 37:4	$[M\text{-}Cl]^+$	68.0	$C_{46}H_{84}O_{22}P_4$	1.8

FOH – fatty alcohol; FA – fatty acid; Cer – ceramide; DG – diacylglycerol; WE – wax ester; PA – phosphatidic acid; PS – phosphatidylserine; PE – phosphatidylethanolamine; TG –triglyceride; PIP – hosphoinositide

https://doi.org/10.17221/159/2024-CJFS

discriminating mutton originating from various geographic locations. Based on the OPLS-DA results, certain specific ions with *m/z* values of 281.194, 702.485, and 723.358 demonstrated the relatively strong discriminatory ability for the geographical origins of lamb. This method eliminates the need for the complex pretreatment of lamb samples. By collecting preliminary data and establishing models, it enables the real-time origin tracing of lamb samples of unknown origin within seconds. However, this technique requires the collection of a large number of authentic samples for modelling purposes. In future, the continuous collection of Qianbei Ma lamb from different ages, body parts, and breeding farms, as well as lamb meat from other regions, will be carried out to refine the model. This is aimed at enhancing the accuracy and reliability of the identification process.

Acknowledgments. All authors are grateful for the help of other colleagues during the course of the study.

REFERENCES

Balog J., Perenyi D., Guallar-Hoyas C., Egri A., Pringle S.D., Stead S., Chevallier O.P., Elliott C.T., Takats Z. (2016): Identification of the species of origin for meat products by rapid evaporative ionization mass spectrometry. Journal of Agricultural and Food Chemistry, 64: 4793–4800.

Birse N., Elliott C. (2024): Rapid evaporative ionisation mass spectrometry for food authenticity and beyond – A review of applications over the first decade (2014–2023). Trends in Food Science & Technology, 144: 104296.

Black C., Chevallier O.P., Haughey S.A., Balog J., Stead S., Pringle S.D., Riina M.V., Martucci F., Acutis, P.L., Morris M., Nikolopoulos D.S., Takats Z., Elliott C.T. (2017): A real time metabolomic profiling approach to detecting fish fraud using rapid evaporative ionisation mass spectrometry. Metabolomics: Official Journal of the Metabolomic Society, 13: 153.

Bodai Z., Cameron S., Bolt F., Simon D., Schaffer R., Karancsi T., Balog J., Rickards T., Burke A., Hardiman K., Abda J., Rebec M., Takats Z. (2018): Effect of Electrode Geometry on the classification performance of rapid evaporative ionization mass spectrometric (REIMS) bacterial identification. Journal of the American Society for Mass Spectrometry, 29: 26–33.

Calvano C.D., De Ceglie C., Aresta A., Facchini L.A., Zambonin C.G. (2013): MALDI-TOF mass spectrometric determination of intact phospholipids as markers of illegal bovine milk adulteration of high-quality milk. Analytical and Bioanalytical Chemistry, 405: 1641–1649.

Camin F., Bontempo L., Perini M., Piasentier E. (2016): Stable isotope ratio analysis for assessing the authenticity of food of animal origin. Comprehensive Reviews in Food Science and Food Safety, 15: 868–877.

Cui Y., Wang H., Zhao Q., Zhu X., Wang, P., Xue, J., Chen, K., Shen, Q. (2021): Real-time detection of authenticity and adulteration of krill phospholipids with soybean phospholipids using rapid evaporative ionization mass spectrometry: Application on commercial samples. Food Control, 121: 107680.

Hiraoka K., Nishidate K., Mori K., Asakawa D., Suzuki S. (2007): Development of probe electrospray using a solid needle. Rapid Communications in Mass Spectrometry: RCM, 21: 3139–3144.

Liu Q., Wu J., Lim Z.Y., Lai S., Lee N., Yang H. (2018): Metabolite profiling of *Listeria innocua* for unravelling the inactivation mechanism of electrolysed water by nuclear magnetic resonance spectroscopy. International Journal of Food Microbiology, 271: 24–32.

Rigano F., Mangraviti D., Stead S., Martin N., Petit D., Dugo P., Mondello L. (2019): Rapid evaporative ionization mass spectrometry coupled with an electrosurgical knife for the rapid identification of Mediterranean Sea species. Analytical and Bioanalytical Chemistry, 411: 6603–6614.

Rui Y., Wang W., Chen L. (2010): Analysis of the composition and concentration of fatty acids in transgenic soybean (cp4-epsps1) oil. Journal of Consumer Protection and Food Safety, 5: 7–10.

Schäfer K.C., Dénes J., Albrecht K., Szaniszló T., Balog J., Skoumal R., Katona M., Tóth M., Balogh L., Takáts, Z. (2009): In vivo, in situ tissue analysis using rapid evaporative ionization mass spectrometry. Angewandte Chemie, 48: 8240–8242.

Shen Q., Wang J., Li S., Rao W., Wang Y., Wang H. (2019): In situ rapid evaporative ionization mass spectrometry method for real-time discrimination of *Pelodiscus sinensis* in different culturing modes without sample preparation. Food Analytical Methods, 12: 2699–2708.

Shen Q., Li L., Song G., Feng J., Li S., Wang Y., Ma J., Wang H. (2020): Development of an intelligent surgical knife rapid evaporative ionization mass spectrometry based method for real-time differentiation of cod from oilfish. Journal of Food Composition and Analysis, 86: 103355.

Song G., Li L., Wang H., Zhang M., Yu X., Wang J., Shen Q. (2020): Electric soldering iron ionization mass spectrometry based lipidomics for in situ monitoring fish oil oxidation characteristics during storage. Journal of Agricultural and Food Chemistry, 68: 2240–2248.

St John E.R., Balog J., McKenzie J.S., Rossi M., Covington A., Muirhead L., Bodai Z., Rosini F., Speller A.V.M., Shousha S., Ramakrishnan R., Darzi A., Takats Z., Leff D.R.

https://doi.org/10.17221/159/2024-CJFS

(2017): Rapid evaporative ionisation mass spectrometry of electrosurgical vapours for the identification of breast pathology: Towards an intelligent knife for breast cancer surgery. Breast Cancer Research: BCR, 19: 59.

Sun S.M., Guo B.L., Wei Y.M., Fan M.T. (2011): Application of near infrared spectroscopy fingerprint analysis in traceability of mutton origin. Spectroscopy and Spectral Analysis, 31: 937–941. (in Chinese)

Verplanken K., Stead S., Jandova R., Poucke C.V., Claereboudt J., Bussche J.V., Saeger S.D., Takats, Z., Wauters J., Vanhaecke L. (2017): Rapid evaporative ionization mass spectrometry for high-throughput screening in food analysis. The case of boar taint. Talanta, 169: 30–36.

Wilde A.S., Haughey S.A., Galvin-King P., Elliott C.T. (2019): The feasibility of applying NIR and FT-IR fingerprinting to detect adulteration in black pepper. Food Control, 100: 1–7.

Zhang J., Ling L., Lu Y., Yang S., Wang L., Xiang L. (2022): Research on the origin traceability of geographical indication protection products Xishui brown goat based on IKnife-REIMS technology. Science and Technology of Food Industry, 43: 286–292. (in Chinese)

Received: August 8, 2024
Accepted: January 28, 2025
Published online: February 25, 2025